

RIGA TECHNICAL UNIVERSITY
Faculty of Power and Electrical Engineering
Institute of Industrial Electronics and Electrical Engineering

Atis HERMANIS

Student of the Doctoral study program "Computer Control of Electrical Technologies"

**SHAPE SENSING BASED ON EMBEDDED SENSORS FOR MOBILE
CYBER-PHYSICAL SYSTEMS**

Summary of the Doctoral Thesis

Academic supervisors
Dr. sc. comp., senior researcher
M. GREITĀNS
Dr. sc. ing., professor
O. KRIEVS

Riga 2016

Hermanis A. Shape Sensing Based on Embedded Sensors for Mobile Cyber-physical Systems. Summary of the Doctoral Thesis.-Riga: RTU press, 2016. – 35 p.

Printed in accordance with the decision of EEF Promotion Council "RTU P-14" on 20th of June, 2016, Protocol No. 2016-3(59).

ISBN 978-9934-10-866-2

**A DOCTORAL THESIS SUBMITTED TO RIGA TECHNICAL UNIVERSITY IN
FULFILLMENT OF THE REQUIREMENTS FOR THE DEGREE OF DOCTOR OF
SCIENCE IN ENGINEERING**

The public defense of the doctoral thesis for promotion to the doctor's degree in engineering will take place on 25th of November, 2016, at 13.00 in Room 212, Institute of Industrial Electronics and Electrical Engineering, Azenes 12/1, Riga.

OFFICIAL REVIEWERS

Professor, Dr. sc. ing. Ilja Galkins
Riga Technical University, Latvia

Professor, Dr. sc. ing. Aleksandrs Grakovskis
Transport and Telecommunication Institute, Latvia

Senior research scientist, Dr. sc. ing. Yannick Le Moullec
Tallinn University of Technology, Estonia

Atis Hermanis (Signature)

Date:

The doctoral thesis is written in English, contains an introduction, 5 chapters, conclusions, references, 7 appendices, an index, 46 figures and one table, 119 pages in total. The list of references consists of 96 titles.

TABLE OF CONTENTS

ABBREVIATIONS	5
GENERAL DESCRIPTION OF THE WORK	6
Urgency of Subject Matter	6
Objective of the Work	6
Methodology of Research.	7
Scientific Novelty and Main Results	7
Thesis Statements to Be Defended	8
Practical Value and Approbation	8
Structure of the Thesis	10
1. METHODS FOR SURFACE SHAPE SENSING WITH EMBEDDED EQUIPMENT.	11
1.1 Shape sensing by measuring bending of the material	11
1.2 Shape sensing by measuring orientation of object segments.	11
1.3 Conclusions	12
2. SHAPE SENSING BASED ON INERTIAL/MAGNETIC SENSOR MODULES	13
2.1 Shape sensing based on accelerometer modules	13
2.2 Shape sensing based on accelerometer and magnetometer modules.	14
2.3 Simulations	16
2.4 Conclusions	18
3. HARDWARE ARCHITECTURE FOR SHAPE SENSING SENSOR NETWORK	19
3.1 Enhanced daisy-chained SPI	19
3.2 Conclusions	20
4. EXPERIMENTAL SYSTEMS	21
4.1 Surface reconstruction with accelerometer network	21
4.2 Sensor network architecture	22
4.3 Surface reconstruction with accelerometer and magnetometer network	23
4.4 Conclusions	25
5. SHAPE SENSING APPLICATION IN MOBILE CYBER-PHYSICAL SYSTEMS.	28
5.1 Posture monitoring and feedback	28
5.2 Approbation and pilots for medical applications	29
5.3 Conclusions	29
DISCUSSION AND CONCLUSIONS.	31
BIBLIOGRAPHY	32

ABBREVIATIONS

2D – *Two Dimensions*
3D – *Three Dimensions*
CLK – *Clock signal*
CPS – *Cyber-Physical Systems*
I2C – *Inter-Integrated Circuit*
MEMS – *Micro Electro Mechanical Systems*
MISO – *Master In Slave On*
MOSI – *Master Out Slave In*
LiDAR – *Light Detection And Ranging*
PC – *Personal Computer*
RGB – *Red Green Blue*
RMS – *Root Mean Square*
SAW – *Surface Acoustic Wave*
SIMO – *Slave In Master Out*
SOMI – *Slave On Master In*
SPI – *Serial Peripheral Interface*
SPP – *Serial Port Profile*
SS – *Source Select*
SWD – *Smart Wearable Device*
TRIAD – *Three Axis Attitude Determination*
UART – *Universal Asynchronous Receiver Transmitter*
USB – *Universal Serial Bus*

GENERAL DESCRIPTION OF THE WORK

The Urgency of Subject Matter

Ability to measure 3D geometric properties of an object can provide data about the shape of the object. If the object is measured in real-time, continuous deformations can also be monitored. This data is valuable for various new emerging applications. Shape sensing ability could be used in robotic systems to gather information about objects in outside environment [1] or to obtain precise feedback of robot manipulator position [2]. In the new emerging field of flexible electronics [3], shape sensing could provide direct feedback of device configuration and allow new ways of interaction with these devices. Additional new fields that are growing very fast and could benefit from shape sensing technologies are wearable computing and smart textiles [4]. Here the data about textile shape could be used to provide real-time information of the wearer's posture and movement. The clear potential applications of shape sensing combined with advancements in new sensing technologies, for example, Micro Electro Mechanical Systems (MEMS) [5], attract more researchers to focus on this field.

The above mentioned applications usually are controlled by a specific group of computers called embedded systems [6]. Historically, embedded systems were treated as small computers and not much distinguished from the general computer science. To control more complex processes, embedded systems had to have closer interaction with the physical world, which introduces new challenges. This encouraged formation of a new embedded system subfield – cyber-physical systems (CPS). CPS can be seen as an extension of embedded systems where the particular focus is on integration of computation with physical processes. Because of this, novel sensing technologies and sensor systems have a huge roll in facilitation of development of new and more functional CPS. In addition, a number of CPS applications such as wearable devices, portable electronics, robotics, etc., often require mobile operation, thus when developing sensor systems for CPS a particular attention have to be paid not only to ensure system operation with limited resources but also ability to work with limited supporting infrastructure.

In relation to CPS, all techniques for 3D shape data acquisition can be divided in two major categories. The first category performs some form of remote sensing utilizing either active or passive external equipment such as single and stereo camera setups, time of flight cameras, LiDARs, touch probes, and other solutions [7]. The second category uses sensors that are placed on or even embedded into the measured object itself. Most of the previous studies that are related to measurement of object 3D geometric properties fall under the first category [8]. These approaches can often provide object models with high accuracy; however, there are two major problems that are inherent in system architecture with external equipment. One is that it requires specially equipped surroundings, which considerably limits the range of operation and portability. The other significant problem is occlusions. External sensors have to have a clear line of sight to the object, which is not always practical. In addition, an object with a more complicated shape can sometimes itself occlude some of its details. Both of these limitations prevent methods with external equipment from being used for mobile CPS applications such as smart shape aware textile, flexible electronics and other; therefore, the focus of this work is on utilization of embedded equipment.

The Objective of the Work

The aim of this work is to facilitate the development of new CPS applications by exploring new 3D free-form shape sensing methods. The focus is on the research of methods utiliz-

ing equipment that enables ubiquitous operation of mobile CPS. Also, attention is paid to the employment of miniature low-cost, low-power hardware, the development of efficient data processing algorithms suitable for real-time CPS, and the development of methods for efficient data acquisition to gather data from a large number of sensors to provide high resolution measurements.

At the beginning of the work the following tasks were defined:

- review the literature related to object shape measurement with sensors embedded in the measured object and identify the most suitable approach for mobile CPS applications;
- develop a shape reconstruction method based on embedded sensors that can obtain real-time 3D shape information and can be implemented in the embedded system;
- develop a method for data acquisition that can effectively gather data from a large number of sensors required by the shape reconstruction algorithm;
- experimentally validate the feasibility of the proposed methods and practically test the shape reconstruction performance;
- implement and approbate the proposed methods in a mobile CPS application.

The Methodology of Research

To complete the tasks of the thesis work, the following research methodology was used. Analytic methods were used for literature review and definition of method architecture. Mathematical calculations and numerical simulations were used to test the feasibility of proposed data acquisition and shape reconstruction algorithms and also to theoretically estimate the impact of different error sources. Experimental testing and measurements were performed to validate data acquisition and shape reconstruction method performance in laboratory environment. Statistical methods were used to quantify the results of experimental tests. Field tests and pilots were done to assess the performance of proposed methods in real-life conditions for medical applications.

Scientific Novelty and Main Results

The main results and scientific novelty of this work is as follows:

- proposed and experimentally validated new method for surface shape reconstruction basing on accelerometer network. Developed new improved approach for accelerometer based shape reconstruction that allows automatic selection of segment direction (rotation around vertical axis) basing on sensor inclination;
- research, development and implementation of a novel method for free-form surface shape reconstruction basing on acceleration and magnetic sensor network data that allows fast computations in embedded systems;
- detailed analysis on the impact of different error sources on shape reconstruction accuracy, as well as practical evaluation of shape reconstruction performance by comparison with state-of-the-art sensor that utilizes external equipment for shape sensing;
- proposed and experimentally validated new method for efficient real-time data acquisition from a wired sensor network with more than 200 hundred sensor nodes that are based on conventional low-power, low-cost electronic components;
- approbation of proposed data acquisition and shape reconstruction methods in mobile CPS for medical application. The system piloted for human posture monitoring in medical study in collaboration with two medical institutions.

Thesis Statements to Be Defended

In this work, the following thesis statements have been promoted and proven:

- low-cost inertial and magnetic sensor network can be used to reconstruct the shape of 3D surface with an average error less than 6 % relative to the smallest surface dimension;
- it is possible to acquire the necessary information about 3D orientation from more than 200 sensors with more than a 50 Hz sampling rate by utilizing the proposed enhanced-daisy chained 4 wire architecture and off-the-shelf hardware;
- the proposed fixed-length vector algorithm allows reconstructing the object shape more than 40 times faster on the same hardware with negligible (less than 1 %) reduction in accuracy compared to state-of-the-art integrating algorithm.

Practical Value and Approbation

The results of this work can be applied for smart textiles for seamless human posture and movement measurements. A system with data acquisition and shape reconstruction methods developed in this work was piloted for human posture monitoring in medical studies. In addition, potential application fields include flexible electronics and robotics where the methods could provide feedback about systems shape.

The results of this work have been published in the following papers:

- A. Hermanis, R. Cacurs and M. Greitans, "Acceleration and Magnetic Sensor Network for Shape Sensing," IEEE Sensors Journal, vol. 16, no. 5, pp. 1271–1280, March 1, 2016. (**Ietekmes koeficients 1.762**, IEEE, Scopus);
- A. Hermanis, R. Cacurs and M. Greitans, "Shape sensing based on acceleration and magnetic sensor system," 2015 IEEE International Symposium on Inertial Sensors and Systems (ISISS), Hapuna Beach, HI, 2015, pp. 1–2. (short paper, IEEE, Scopus);
- K. Nesenbergs, A. Hermanis, M. Greitans, "A Method for segment based surface reconstruction from discrete inclination values", (2014) Elektronika ir Elektrotehnika, vol. 20, no. 2, pp. 32–35. (Scopus);
- A. Hermanis, R. Cacurs, K. Nesenbergs and M. Greitans, "Efficient real-time data acquisition of wired sensor network with line topology," 2013 IEEE Conference on Open Systems (ICOS), Kuching, 2013, pp. 133–138. (IEEE, Scopus);
- A. Hermanis, K. Nesenbergs, R. Cacurs, and M. Greitans, "Wearable Posture Monitoring System with Biofeedback via Smartphone", Journal of Medical and Bioengineering vol. 2, no. 1, pp. 40–44, 2013. (WorldCat, CrossRef);
- A. Hermanis and K. Nesenbergs, "Grid shaped accelerometer network for surface shape recognition," 13th Biennial Baltic Electronics Conference, Tallinn, 2012, pp. 203–206. (**Best Paper Award**, IEEE, Scopus).

The results of this work have been published in the following conference abstracts, demos and posters:

- A. Hermanis, R. Cacurs, K. Nesenbergs, M. Greitans, E. Syundyukov, and L. Selavo. 2016. Demo: Wearable Sensor System for Human Biomechanics Monitoring. In Proceedings of the 2016 International Conference on Embedded Wireless Systems and Networks (EWSN '16), 15–17 February. Gratz, Austria. Junction Publishing, USA, 247–248. (Demo, abstract and poster, ACM);
- A. Hermanis, R. Cacurs, K. Nesenbergs, M. Greitans, E. Syundyukov, L. Selavo, "Wearable sensor grid architecture for body posture and surface detection and rehabilitation", (2015) IPSN 2015 – Proceedings of the 14th International Symposium on Information

Processing in Sensor Networks (Part of CPS Week), pp. 414–415. (Demo, abstract and poster, ACM, Scopus);

- A. Hermanis, A. Greitane, S. Geidane, A. Ancāns, R. Cacurs, M. Greitans, "Wearable Head and Back Posture Feedback System For Children With Cerebral Palsy", Abstract: Journal of Rehabilitation Medicine (ISSN 1650-1977), 2015. (Abstract);
- K. Nesenbergs, A. Hermanis, A. Greitane, M. Greitans, "Virtual Reality Rehabilitation System for Children with Cerebral Palsy", 25th European Academy of Childhood Disability, Newcastle, England, 10–12 October, 2013. (Poster);
- A. Hermanis, K. Nesenbergs, "Accelerometer network for human posture monitoring", Riga Technical University 53rd International Scientific Conference, 10-12 October, 2012 Riga. (Abstract).

The results have been promoted in the following international conferences and workshops:

- "4th Baltic and North Sea Conference on Physical and Rehabilitation Medicine", 16–18 September 2015, Riga, Latvia;
- "Cyber-physical systems week 2015", 13–16 April 2015, Seattle, WA, USA;
- "2015 IEEE International Symposium on Inertial Sensors and Systems (ISISS)", 23–26 March 2015, Hapuna Beach, USA;
- "2013 IEEE Conference on Open Systems (ICOS)", 2–4 December 2013, Kuching, Malaysia;
- "2013 2nd International Conference on Medical Information and Bioengineering (ICMIB 2013)", 16–17 March 2013, Bali, Indonesia;
- "International Symposium on Biomedical Engineering and Medical Physics", 10–12 October 2012, Riga, Latvia;
- "13th Biennial Baltic Electronics Conference", 3–5 October 2012, Tallin, Estonia;
- "5th International Doctoral School of Energy Conversion and Saving Technologies", 27–30 May 2016, Ronisi, Latvia;
- "4th International Doctoral School of Electrical Engineering and Power Electronics", 29–30 May 2015, Ronisi, Latvia;
- "3rd International Doctoral School of Electrical Engineering and Power Electronics", 23–24 May 2014, Ronisi, Latvia;
- "2nd International Doctoral School of Electrical Engineering and Power Electronics", 24–25 May 2013, Ronisi, Latvia;
- "From exclusion to inclusion" Conference on novelties in Cerebral Palsy research, University of Latvia, May 8th 2014, Riga, Latvia;
- Latvijas Ergoterapeitu asociācijas vasaras konference 2014 "Ergoterapijas prakses kontekstu daudzveidība – mūsdienīgas metodes ergoterapijā", 14. jūnijs, 2014. g., rehab. centrs "Vaivari", Jūrmala, Latvija;
- Summer School "Smart Textiles for Healthcare", 25–28 August 2015, Riga, Latvia.

The work has been implemented in the Institute of Electronics and Computer Science, Riga, Latvia, and the results have been applied in the following projects:

- National Research Program „Cyber-physical systems, ontologies and biophotonics for safe and smart city and society” (SOPHIS) project No. 1 „Development of technologies for cyber physical systems with applications in medicine and smart transport” (KiFiS);
- European Social Funds project "Smart City Technologies for Human Lives Improvements" (ViPTeh) No. 2013/0008/1DP/1.1.1.2.0/13/APIA/VIAA/016;
- State Research program "Development of innovative multi-functional material, signal processing and information technologies for competitive and research intensive products" project No.2 "Innovative signal processing technologies for smart and effective electronic system development" (IMIS).

Structure of the Thesis

The volume of the Thesis is 118 pages, and it has following structure.

In Section 1, a detailed literature review of various shape sensing methods that are based on embedded equipment is provided. The most suitable approach for mobile CPS is identified. In Section 2, methods for 3D shape reconstruction based on local orientation data are proposed. First, a case with application of acceleration sensor network together with its limitations is described. Then a method utilizing acceleration and magnetic field sensor network is proposed. Detailed simulations are provided to validate the feasibility of this method. In Section 3, various communication interfaces available for integral circuits are reviewed and a new method is proposed for an effective data acquisition from a large number of sensors suitable for shape sensing applications. Section 4 is dedicated to the description of development and testing of experimental systems for shape sensing sensor network. Detailed shape reconstruction performance evaluation of the proposed method is provided here. In Section 5, the implementation and approbation of proposed methods in mobile CPS is shown. A mobile posture monitoring device for medical applications that is based on new the methods proposed in this work is demonstrated. An approbation in medical institutions for patients with posture and movement dysfunction is also described. At the end of the work, overall discussion and conclusions are given.

This Doctoral thesis is based on the papers **[9, 10, 11, 12, 13, 14]** by the author of this Thesis and paper co-authors Ricards Cacurs, Modris Greitans, and Krisjanis Nesenbergs. Some additional information found in this work is previously published in a Master's thesis work **[15]** by the author of this work and in the conference abstracts and demos **[16, 17, 18, 19, 20]** with additional co-authors Armands Ancans, Emil Syndykov, Leo Selavo, Santa Geidane and Andra Greitane. Here and further in the text, the references with authors own contribution are highlighted in bold and underlined.

1. METHODS FOR SURFACE SHAPE SENSING WITH EMBEDDED EQUIPMENT

In the literature, a number of studies try to acquire a 3D shape of object surface by utilizing sensors that can be placed on the object or even embedded into the object. These are often referred as self sensing devices as they include the required sensors themselves. Usually, a network of sensors is used to provide some local information from multiple locations on the object, which can then be used together to obtain global shape characteristics. These studies can be categorized in two major subgroups.

1.1. Shape sensing by measuring bending of the material

In one subgroup, the information about object shape is obtained by measuring the bending of the material basing on various physical principles that can be sensed by an electronic equipment [21]. Some form of shape sensing has been proposed by different types of bend sensors: surface acoustic wave sensors [22], fiber optic sensors [23], piezoelectric sensors on polymer substrates [24, 25] as well as embedded into fabric [26].

Most of the surface shape sensing methods that are based on measurement of material bending have similar properties. The most frequently mentioned problems include hysteresis of the sensors, aging, limited resolution, complex hardware and data processing algorithms to provide information about deformations with high degree of freedom in larger surface areas. Also, a lot of focus is on recognition of discrete deformations rather than on universal full free-form 3D shape reconstruction. This is partly because of the complexity of mapping the raw sensor readings to precise continuous deformations due to various sensor errors and other effects described earlier.

1.2. Shape sensing by measuring orientation of object segments

In other subgroup, the shape of the object is estimated by measuring orientation of different shape segments. The global shape characteristics are reconstructed from the local orientation information basing on known interconnection model between the segments. Recent advances in MEMS technologies [5] allow manufacturing miniature low-cost inertial sensors that can be used for orientation estimation.

Most of previously proposed shape sensing methods that are based on orientation measurement with inertial sensors are used for specific non-general purposes. Most popular application examples include wearable systems that allow monitoring of different poses and movements of human body [27, 28, 29, 30, 31]. In these works, the sensors are attached to various parts of human body and the pose of the body is reconstructed using biomechanical models.

In contrast only a few researchers have tackled the problem of reconstructing free form shape from inertial/magnetic sensors in general case. In [32, 33], the authors propose a basic surface shape reconstruction with three-axis accelerometer network. In [34, 35], a network of 3-axis acceleration/magnetic sensors is used to reconstruct surface, but only superficial method description is given. Authors in [36, 37] describe their work on 3D curve reconstruction from orientation measurements. In [38, 39], multiple such curves are applied for surface reconstruction, and continuous animation is demonstrated in [40]. The methods rely on detailed data interpolation between the sensor nodes and are mathematically non-trivial requiring relatively high processing power for implementation on portable devices. Also, difficulty to provide reference for shape reconstruction accuracy evaluation as well as complicated data acquisition process

to obtain real-time measurements are reported. Because of this, practical implementation and system performance is not tested in detail.

In many of the aforementioned works, accelerometers are supplemented with magnetic sensors in order to measure an additional reference vector and provide complete 3D sensor orientation estimate [41] that allows reconstructing full 3D shape model. Additionally, gyroscopes often are added to the system to provide accurate orientation estimates in dynamic conditions and when mechanical vibrations occur [42]. Accelerometers mainly have high frequency noise that occurs due to the highly dynamic movements and vibrations. In contrast, gyroscope based orientation measurement have mainly low frequency noise often referred as drift [43]. To utilize this complimentary nature, a number of filters have been proposed [44, 45, 46, 47]. Despite the advantages that gyroscopes can provide, significantly more complicated data processing is required. Also, in modern MEMS low-power systems gyroscopes can consume over 17 times more current than accelerometers and magnetometers combined [48].

1.3. Conclusions

There are a number of studies that are dedicated to 3D shape acquisition with embedded equipment; however, many of these just provide superficial method descriptions leaving important details not yet resolved, which limits validation and practical implementation.

Bend sensors usually provide the data regarding only single degree of freedom of deformation requiring to design complicated sensor networks to measure non-trivial 3D shapes. Also, various physical imperfections of these sensors such as hysteresis, nonlinearity and aging makes the development of signal processing algorithms cumbersome. These drawbacks provide difficult application of these methods in mobile CPS.

The most successful solutions utilizing orientation measurements are designed for specific non-general applications. A very limited previous work has been done to implement and experimentally validate this approach for general case free-form shape measurements such as acquisition of the shape of the surface. This is mainly due to the problems related to design of sensor network for effective data acquisition and relatively complicated data processing algorithms for orientation measurements. Despite this, high degree of freedom measurement, highly efficient production of MEMS and easy integration in the embedded systems make this approach very promising. Because of this, the author further in this work chooses to study shape sensing based on orientation measurements from inertial/magnetic sensors. From inertial sensors only the accelerometers are considered, because gyroscopes consume significantly larger amount of current and have resource intensive signal processing requirements.

2. SHAPE SENSING BASED ON INERTIAL/MAGNETIC SENSOR MODULES

2.1. Shape sensing based on accelerometer modules

Any orientation of a rigid body can be represented as a rotation of the body reference system within the global reference system. A popular way to represent an orientation is with the rotation quaternions [49]. In short, the quaternion representation defines one rotational axis \vec{n} and one rotation angle θ .

In static conditions normalized 3-axis accelerometer measurement vector $(a_x; a_y; a_z)$ can be defined as a vertical vector $(0; 0; 1)$, which has been rotated by an angle θ about an axis $(a_x; a_y; a_z)$ relative to some global reference system. Angle θ and rotation axis \vec{n} can be obtained by:

$$\theta = \arccos((a_x; a_y; a_z) \cdot (0; 0; 1)). \quad (2.1)$$

$$\vec{n} = (a_x; a_y; a_z) \times (0; 0; 1). \quad (2.2)$$

Components of rotation quaternion can be obtained as follow:

$$\begin{aligned} q_0 &= a = \cos\left(\frac{\theta}{2}\right) \\ q_1 &= n_x b = n_x \sin\left(\frac{\theta}{2}\right) \\ q_2 &= n_y b = n_y \sin\left(\frac{\theta}{2}\right) \\ q_3 &= n_z b = n_z \sin\left(\frac{\theta}{2}\right). \end{aligned} \quad (2.3)$$

Rotation quaternion can be applied directly to transform 3D vectors, or used to construct classic three by three rotation matrix $R(q)$ [49]. $R(q)$ represents rotation that describes sensor orientation in relation to global reference frame. Any vector describing surface segment can be simply transformed by multiplying it with $R(q)$:

$$\vec{v}' = R(q)\vec{v}, \quad (2.4)$$

where \vec{v} is the vector and \vec{v}' is the same vector transformed according to sensor orientation.

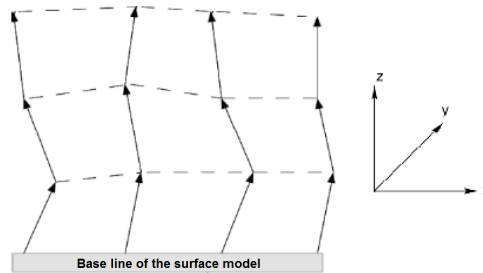


Figure 2.1. Structure of reconstructed surface model.

To reconstruct the shape of the actual sensor network, first the orientation matrix $R(q)$ of each sensor is obtained [14]. Then the rotation matrices are used in the equation (2.4) to transform the corresponding surface segments represented by the vectors to the actual orientation of the corresponding sensor (Fig. 2.1).

One must note that the rotation matrix includes only two degrees of freedom: roll and pitch. Rotations along the third degree of freedom can not be obtained from inclination measurements and are assumed to be zero in this model. This simplification allows a basic shape approximation, but can introduce significant errors in more complicated surface shapes.

To minimize this drawback, a method is proposed for minimization of segmented surface approximation error by selection of z-axis rotation angle for each segment if only inclination of each segment is known [13]. A surface consisting of I equal size segments arranged in an evenly spaced $n \times m$ grid formation is assumed. Each segment in the model is represented as a cross-shaped object defined by four direction vectors. Starting data $\vec{N}_i, \vec{E}_i, \vec{S}_i, \vec{W}_i$ for each $i \in [1, \dots, I]$ segments are calculated by rotating vectors $\vec{N}, \vec{E}, \vec{S}, \vec{W}$ to the inclination values of the corresponding segment measured by sensor. The actual segment z-axis rotation angle α_i and actual segment center vector \vec{C}_i are calculated by dividing the shape reconstruction into $(n - 1) \cdot (m - 1)$ sub-problems, hereinafter referred to as work-sets. Each of these work-sets consist of four segments A1, A2, A3, A4, which are connected in such a way that without any initial rotation they would form a square as seen in Fig. 2.2.

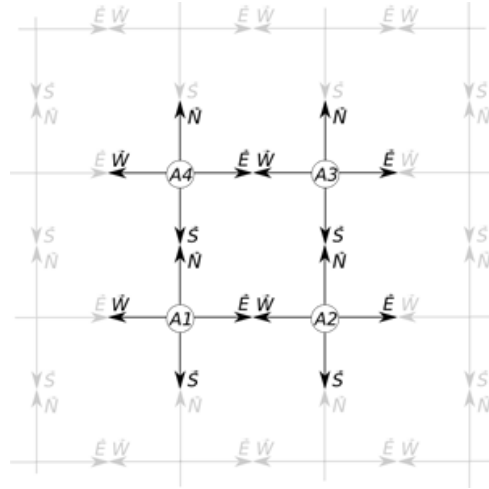


Figure 2.2. Structure of a work-set.

Within a work-set, three of four pairs of segments are assumed to be jointed in “U” shaped pattern forming an equation system:

$$\begin{cases} \vec{C}_{A1} + \vec{E}_{A1} = \vec{C}_{A2} + \vec{W}_{A2} \\ \vec{C}_{A1} + \vec{N}_{A1} = \vec{C}_{A4} + \vec{S}_{A4} \\ \vec{C}_{A2} + \vec{N}_{A2} = \vec{C}_{A3} + \vec{S}_{A3}. \end{cases} \quad (2.5)$$

Initially, one of the segments is defined to serve as a reference for the rest of the model. Then the algorithm evaluates all the combinations of possible successive discrete α_i values from a certain interval within the work-set of this segment using exhaustive search algorithm. In each combination, the matching error Δ_d between the forth segment pair in the work-set is calculated. Assuming continuous surface, the combination with lowest Δ_d is considered the best. After α_i and \vec{C}_i of the work-set segments have been obtained, the next work-set is chosen so that it contains at least one previously processed segment.

This proposed improvement has limitations in the general case, when inclination and restricted model do not provide enough information for selection of segment vertical rotations.

2.2. Shape sensing based on accelerometer and magnetometer modules

For a detailed free-form 3D shape measurement, a system based on orientation measurements of acceleration and magnetic field sensor network was developed.

As stated previously, orientation can be described with the rotation matrix R . The problem of finding R is discussed a lot in spacecraft attitude estimation, where R can be found using observations of the Sun and star directions [50, 51]. The same problem can be assigned also to determine the orientation of the sensor node that can measure the Earth's gravity and magnetic field vectors. The general problem of orientation determination can be stated as Wahba's problem [52], which seeks the R as the solution for minimization of the expression:

$$\sum_{k=1}^K \|v_k^* - Rv_k\|^2, \quad (2.6)$$

where $\{v_1, v_2, \dots, v_K\}$ and $\{v_1^*, v_2^*, \dots, v_K^*\}$ are the sets of K vector observations in object and general reference frames respectively. Acceleration/magnetic sensors provide only two vector observations at each system state, which is minimum for full orientation determination with deterministic approach. Because of this, no real minimization problem can be defined. Several algorithms exist that can obtain orientation from two vector measurements [41, 53].

The TRIAD [41] was used as one of the fastest, singularity free and computationally simple deterministic algorithms for orientation estimation. By applying to TRIAD algorithm, Earth's gravity and magnetic field direction measurements in sensor reference frame and the reference directions of these vectors in the Earth's reference frame, a rotation matrix R that describes full 3D orientation of sensor relative to the Earth's reference frame is obtained. Rotation matrix R can then be used as the relative surface segment orientation. Any vector describing surface segment can be simply transformed by multiplying it with R :

$$\vec{v}' = R\vec{v}, \quad (2.7)$$

where \vec{v} is the vector in initial state in the shape model, and \vec{v}' is the same vector transformed according to sensor orientation.

The problem of reconstruction of free-form 3D shape from full three-degree of freedom local orientation data have not been previously studied in detail. State-of-the-art approach is to treat the orientation information as local tangent data of the surface [36, 38]. In essence, the tangent data provide discrete samples of the curve derivatives. By knowing the derivative sample values and the curvilinear distances (arc lengths) between them, an equation can be formed:

$$L = \int_{p_k}^{p_{k+1}} \|U'(l)\| dl, \quad (2.8)$$

where $U(l)$ is a curve parameterized by an arc length parameter l with known derivatives $U'(l)$ at points $l = p_k$ ($k = 1, \dots, n$), where n is the total number of sensor nodes; $L = p_{k+1} - p_k$ is the distance between the sensor nodes assuming an even sensor distribution. The shape of the curve is reconstructed by first interpolating the discrete derivative samples to obtain continuous $U'(l)$ (preserving the relation in equation (2.8)). Then $U'(l)$ is numerically integrated to obtain the curve solution. Reconstruction of multiple curves can provide surface shape data.

Due to the requirement for the interpolation and numerical integration, the method requires a considerable computing power. Also, curvatures with the period less or equal to the distance between the sensors can not be reconstructed limiting the benefits of accurate interpolation and integration and increasing the requirements for more and densely spaced sensors.

Basing on state-of-the-art approach, a new algorithm was designed with the emphasis on the

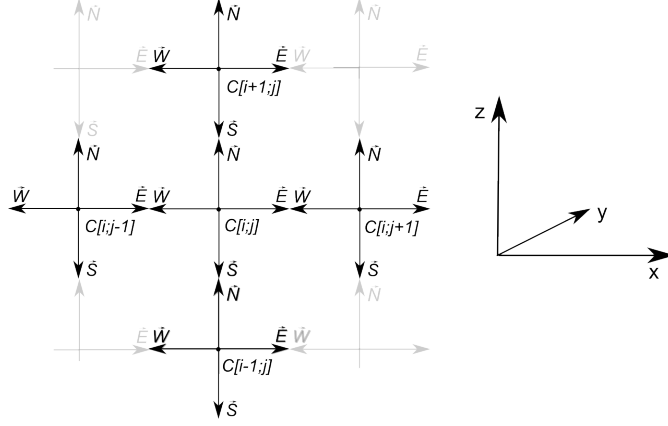


Figure 2.3. Surface segment structure.

Each segment consists of center C and four direction vectors \vec{N} , \vec{E} , \vec{S} and \vec{W} .

application of as many sensors as possible to increase resolution and decrease computing time [9, 10]. Instead of detailed interpolation and integration, it is assumed that sensors are attached to a rigid mutually connected segments of the surface. This provides a coarser approximated model, but can noticeably decrease the computing time. The approach allows fast shape reconstruction from a large number of sensors, which provides a higher sensor density thus increasing the resolution and overall performance of shape reconstruction.

The model of the surface is divided in n rigid segments, where $n = i \cdot j$ is the total number of sensors used, so that the segment structure corresponds to the structure of the sensor grid (i and j denote the row and column of sensor location in the grid). Each segment is described by four direction vectors, denoted by $\vec{N}[i; j]$, $\vec{E}[i; j]$, $\vec{S}[i; j]$, and $\vec{W}[i; j]$, and segment center point $C[i; j]$ as shown in Fig. 2.3. The segment center points define the surface geometry. Initially, all segments are aligned with the global reference system by assigning some base direction vector values: $\vec{N}_b = (0; 0; \frac{L_1}{2})$; $\vec{E}_b = (\frac{L_2}{2}; 0; 0)$; $\vec{S}_b = (0; 0; -\frac{L_1}{2})$; $\vec{W}_b = (-\frac{L_2}{2}; 0; 0)$. L_1 is the distance between sensors lengthwise, and L_2 is the distance between sensors across in the actual grid.

During shape reconstruction, the base direction vectors are translated according to the corresponding sensor orientation using equation (2.7). Segment structure (Fig. 2.3) shows that if a single center point location is known, then any other center point on the same row or column can be calculated by adding and subtracting the corresponding segment direction vectors.

Paths along rows or columns can be used to calculate the segment center point locations (Fig. 2.4). Both cases should provide equal outcome; however, the results may differ depending on the chosen connection path due to the finite number of sensing elements in the grid and measurement errors. To overcome this problem during the control point reconstruction, an averaged values from both cases are used as the surface control point coordinates to form a closed grid.

The obtained control points can be seen as a 3D point cloud defining the shape of the body similar to a 3D scanner. The full shape model is constructed by drawing a quad-mesh structure through control points that coarsely approximate the surface shape. If high sensor density is used, this method can provide reasonably smooth models.

2.3. Simulations

The proposed shape approximation method was compared to the state-of-the-art approach [36]. For simplification purposes, only 2D case was analyzed. A complex curve similar as

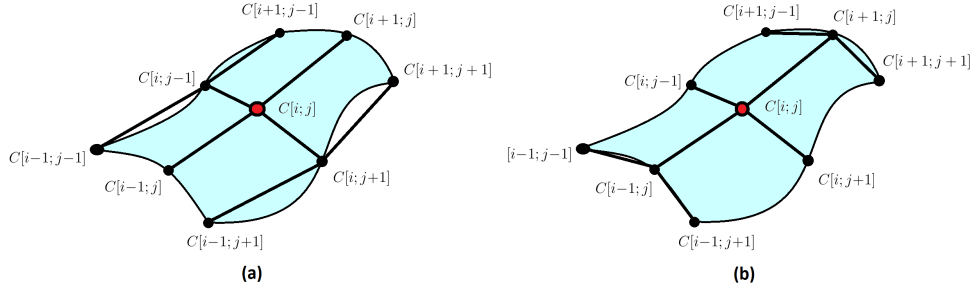


Figure 2.4. Structure of control point connections.

$C[i; j]$ – reference point; (a) single reference row is obtained, then all other points are calculated with column method; (b) single reference column is obtained, then all other points are calculated with row method.

in [36] was synthesized [9]. The curve was reconstructed from 30 simulated sensor locations with proposed method and method described in [36] (Fig. 2.5). The average Euclidean distance between reference and reconstructed sensor locations relative to curve length with proposed method and method in [36] was 0.49 % and 0.31 % respectively. Simulation was done in MATLAB on 3.2 MHz dual core PC, and the calculation times were measured 0.72 ms for the proposed method and 30.05 ms for the method in [36].

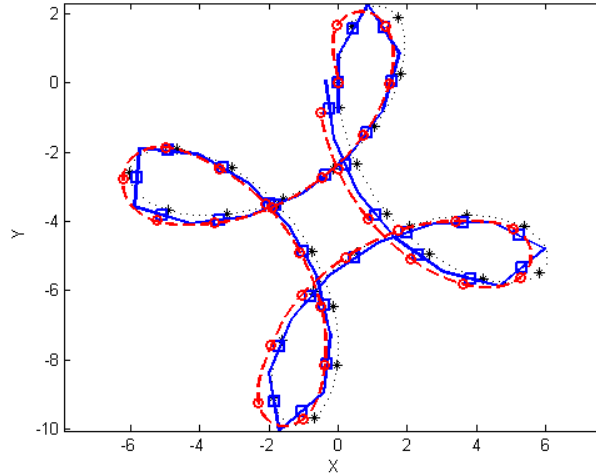


Figure 2.5. Comparison of reconstruction methods.

The synthesized curve is the dotted line with stars indicating sensor locations. Reconstruction of [36] is the dashed line with circles indicating sensor locations. The proposed method is the solid line with squares indicating sensor locations.

In addition to approximation errors, a number of different error sources arise from measurement process. To estimate the impact of each error source on shape reconstruction accuracy, nine sensor nodes evenly distributed along 3D curve were synthesized and theoretical acceleration and magnetic sensor readings were obtained. In Fig. 2.6, the synthesized curve is the dotted line with stars indicating simulated sensor locations. The reconstructed curve is the solid line, the sensor locations are denoted by squares. Before reconstruction, the theoretical acceleration and magnetic sensor data were deteriorated with different errors with increasing magnitudes to observe the impact on reconstruction accuracy. For each error source with each standard deviation, 1000 Monte Carlo runs were performed. Mean values of average reconstruction errors are depicted in Fig. 2.7. For each curve, ε denotes the value of simulated error standard deviation

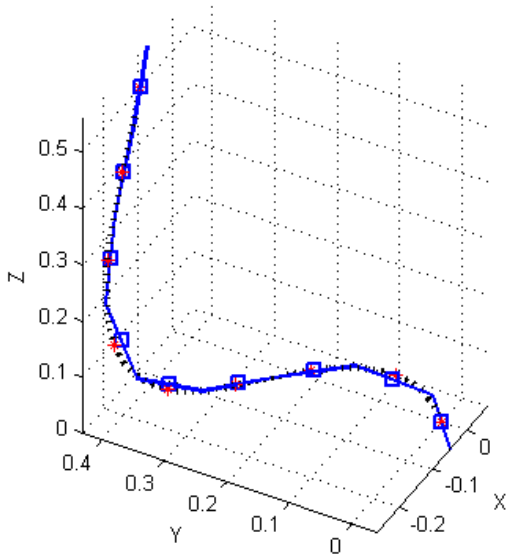


Figure 2.6. Synthesized 3D curve.

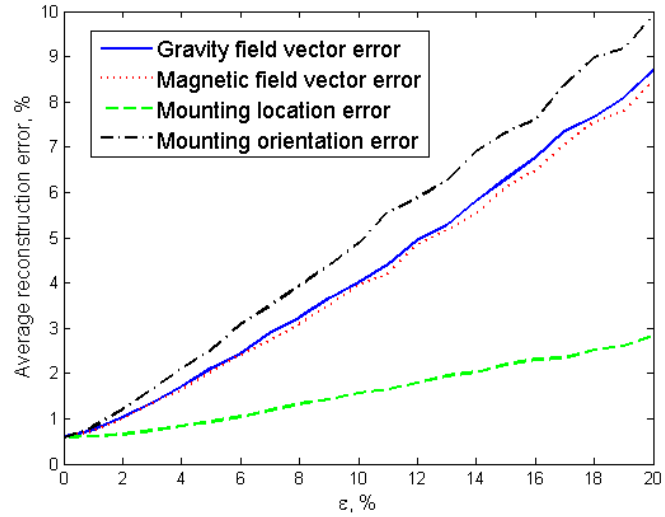


Figure 2.7. Impact of various error sources.

relative to: gravity field vector length; magnetic field vector length; distance between sensors (mounting location error), π (mounting orientation error). The average curve reconstruction error using undeteriorated data (approximation error) was 0.59 % relative to curve length.

2.4. Conclusions

The main advantage of the surface reconstruction with acceleration sensors solely is more simple data processing and system structure with only one type of sensors. To obtain free-form 3D shape data, a method that is based on full 3 degree of freedom orientation measurements is beneficial. It is demonstrated that the proposed shape approximation approach with finite length vectors compared to previously proposed detailed interpolation and integration of local derivatives provides reconstruction more than 40 times faster (Matlab simulation), while providing only a slightly lower reconstruction accuracy. Due to the inability of interpolation algorithms to estimate deformations with the period smaller than or equal to the distance between sensors, to obtain a higher shape sensing resolution and accuracy, the density of the sensors has to be increased. Therefore, it seems that for practical real-time shape sensing systems the complicated reconstruction algorithms can be substituted with simplified approximation in favor of faster processing time that allows higher sensor density. The clear limitation of the method is sensor spatial density which has to be as high as possible to measure deformations with small period.

3. HARDWARE ARCHITECTURE FOR SHAPE SENSING SENSOR NETWORK

3.1. Enhanced daisy-chained SPI

Data acquisition from shape sensing sensor network is a challenging task as it benefits from a large number of sensors. Also data transfer interface has to have a simple wiring structure to reduce the amount of wires, a limited power consumption, a reasonable data transfer speed, and a limited size of hardware implementation. Conventional data transfer interfaces available in current low-power microelectronics are not directly suitable for this task; also, existing solutions for large scale networks with advanced addressing and routing cannot be applied effectively due to limited resources. Because of this, a new solution for data acquisition with custom network interface was developed [11]. The method supports up to several hundred sensors and can be implemented using conventional low-cost hardware with a simple four wire serial connection.

The proposed solution is based on daisy-chained SPI [54]. Instead of connecting each slave to the clock line in parallel, the clock signal is repeated in every slave (Fig. 3.1). The signal repeater acts as a buffer for each stage of the clock line, thus removing effects from the rest of the clock circuit. This solution reduces the network to multiple relatively simple and independent links between two adjacent sensor nodes in the chain. The whole network can be formed with only 4 wires in total: 2 communication lines which connect sensors in series, and 2 parallel power supply lines.

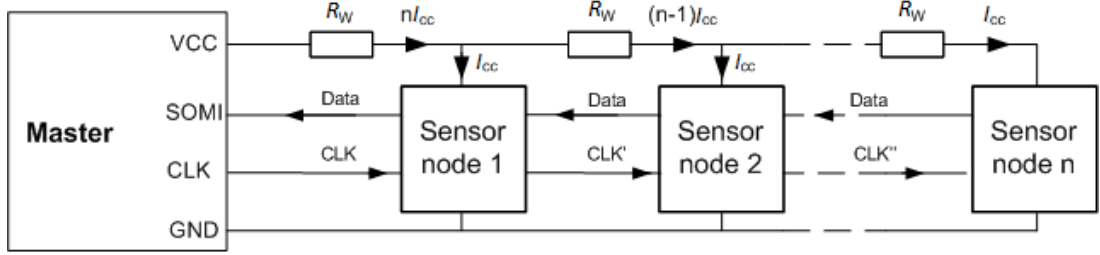


Figure 3.1. Structure of enhanced daisy-chained SPI network.

The clock signal repetition can be achieved with an analogous comparator integrated into many low-power mixed signal microcontrollers reducing the requirement for additional hardware components. As the clock signal has non-ideal edges, the pulse width of the repeated signal T_{ref} can vary depending on the comparator reference voltage V_{ref1} . This is depicted in Fig. 3.2, where $T_{ref1} < T_p < T_{ref2}$. T_p is the incoming clock signal width. After multiple signal repetitions, the signal gets too distorted for SPI module to work properly. An automatic calibration is proposed which at each sensor node measures the incoming clock signal positive pulse width, and decides which reference to use depending whether the signal positive pulse width needs to be expanded or narrowed.

One of the limitations of the proposed architecture is the voltage drop on power lines which can be estimated by:

$$V_n = V_{cc} - \sum_{k=1}^n k I_{cc} R_W, \quad (3.1)$$

where V_n – supply voltage on last sensor node [V]; V_{cc} – master power supply voltage [V]; I_{cc} – current consumption per sensor node [A]; R_W – wire resistance between two sensor nodes [Ω]. Basing on minimum required V_n , equation (3.1) can be used for estimation of maximum number of sensors.

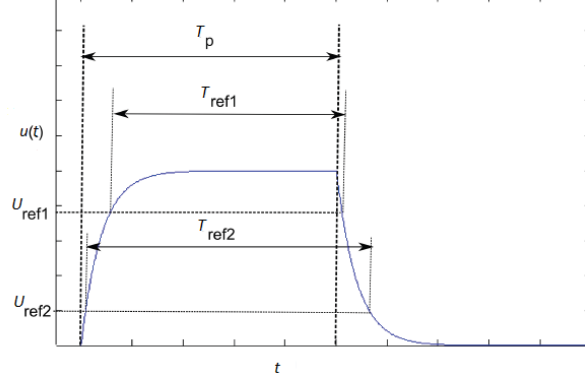


Figure 3.2. Clock pulse width variance with different comparator reference signals.

Other property that limits maximum number of sensors is the application required sampling rate of each sensor in the network. It can be estimated by:

$$T_{\text{sample}} = bn \left(\frac{8}{f_{\text{CLK}}} + T_{\text{SPI}} \right) + T_{\text{data}}, \quad (3.2)$$

where T_{sample} – minimum sampling period [s]; f_{CLK} – SPI clock signal frequency [Hz]; n – number of sensor nodes in network; b – number of bytes from each sensor; T_{data} – delay for data preparation in sensor node [s]; T_{SPI} – SPI hardware related delay.

3.2. Conclusions

The proposed method can provide efficient data acquisition of multi-sensor network by connecting devices in line topology. This allows overcoming the addressing problems that occur in networks with a large number of nodes. The method also reduces the number of wires and provides a simple wiring structure for convenient integration into the garment. The simple wire structure also is beneficial for e-textiles that can substitute wires with conductive yarns [55]. At the same time, the method requires only conventional low-power hardware and provides reasonable data transfer speeds for real-time systems, which are essential aspects in a number of applications.

The enclosed microcontrollers can also be used to do data pre-processing and create systems with a distributed computing architecture. This can provide significant benefits for real-time, low-power applications in mobile CPS.

4. EXPERIMENTAL SYSTEMS

4.1. Surface reconstruction with accelerometer network

To validate the performance of the surface shape reconstruction from accelerometer sensor data described in Subsection 2.1, a prototype device was built consisting of a 3-axis accelerometer network and a data acquisition board [14, 15] (Fig. 4.1). A network of 16 accelerometers organized in a 4×4 -grid configuration was used.

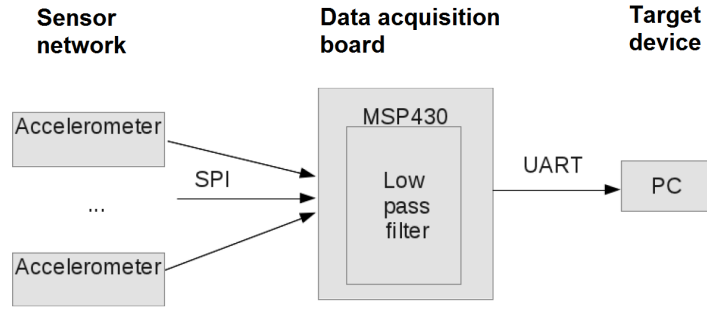


Figure 4.1. Structure of the experimental accelerometer system.

The shape reconstruction accuracy was tested by applying sensor grid to different surfaces with known geometry. Test shapes were chosen with relatively simple deformations where the orientation detection of the sensors around vertical axis is not required. The average sensor location reconstruction error was 0.71 cm.

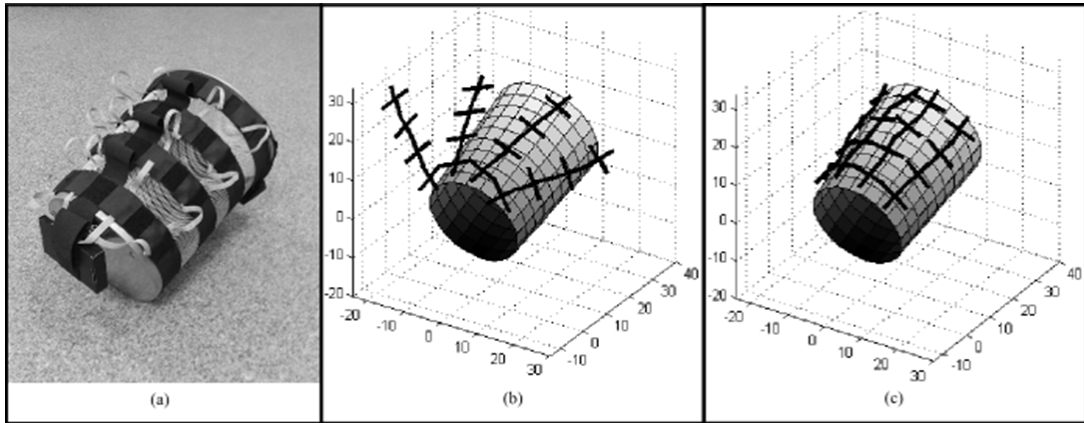


Figure 4.2. Experimental test setup of accelerometer network.

a) experimental model; b) superimposed reference object and reconstructed surface model assuming fixed segment orientations around vertical axis; c) superimposed reference object and reconstructed surface model with estimation of orientations around vertical axis.

To experimentally test the feasibility of the proposed method that allows selection of rotation angle for third degree of freedom (rotations around vertical z-axis) basing only on inclination data, the sensors were fixed on a curved reference surface [13]. In Fig. 4.2, the comparison between reconstruction using the method with fixed segment z-axis rotation and with the method that provides estimation of these rotations is shown. A noticeable improvement can be seen, but the reconstruction time in the latter case was approximately 1 second on a modern personal

computer with the algorithm implemented in Matlab environment limiting the application on systems with limited resources.

4.2. Sensor network architecture

To validate the enhanced daisy-chained SPI proposed in Subsection 3 that would allow data acquisition from a large number of sensors, an experimental proof-of-concept setup was developed with 60 sensor nodes (Fig. 4.3) [11]. All nodes were connected in a chain with point-to-point connections according to the structure in Fig. 3.1.

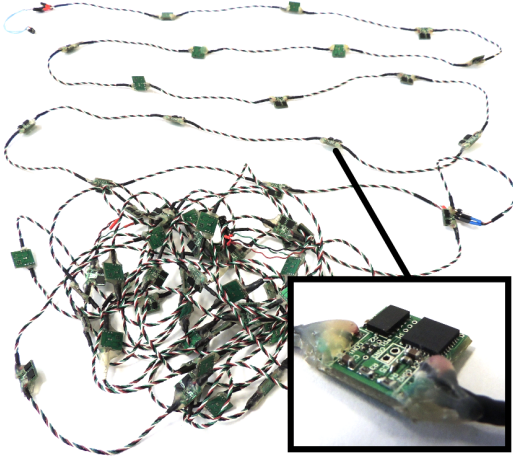


Figure 4.3. Experimental sensor chain with 60 sensor nodes.

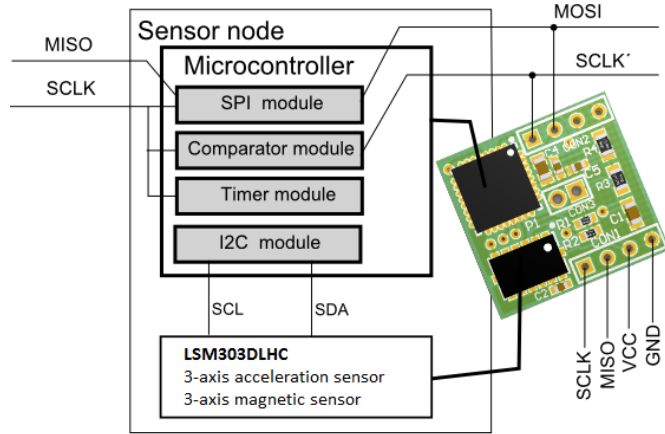


Figure 4.4. The structure of the sensor node (dimensions: 13 mm × 13 mm × 2 mm).

In the experimental setup, the MSP-EXP430FR5739 development board was used as the master device. For the sensor nodes, the 3-axis acceleration and magnetic sensors LSM303DLHC communicating over I2C line to the MSP430g2553 microcontroller were used (Fig. 4.4).

The clock signal repetition on sensor node is done by the comparator built in the microcontroller. As described in the Subsection 3, the repeated clock signal width gets distorted in each repetition and specific calibration is required. The calibration is provided by connecting incoming clock signal to the timer module that can measure the clock signal pulse width. According to the pulse width, a comparator reference value is selected so that it compensates any distortion in the clock signal pulse width.

In the experimental setup, master supply voltage V_{cc} was 3.6 V. The measured supply current RMS value of each sensor node I_{cc} was 460 μ A resulting in overall current consumption of all 60 sensor network to 27.6 mA. The wire resistance R_w was measured 0.15 Ω . The curve in Fig. 4.5, obtained using equation (3.1), illustrates the relationship between the number of sensors in the network and the last sensor supply voltage for network with these parameters. Theoretical supply voltage on last sensor node for the 60 sensor network is marked as 3.47 volts and approximately corresponds to that experimentally measured. Based on minimum power supply requirement for the sensor LSM303DLHC which is 2.18 V, the maximum number of 201 sensor nodes is estimated for this setup.

The SPI data transfer clock frequency was 1 MHz. The experimentally determined data preparation time T_{data} was 200 μ s. The measured SPI hardware delay was approximately 8 μ s. Inserting these parameters into the equation (3.2), the minimum sampling period was calculated as 6 ms, which corresponds to around 166 Hz sampling rate for 60 sensor network with 6 bytes to receive from each sensor node. Based on the same calculations, a maximum sampling rate for the

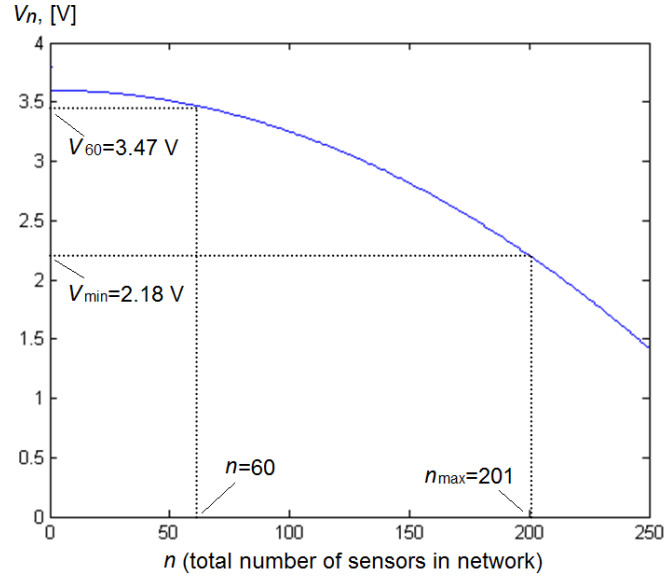


Figure 4.5. Relation between the number of sensors in the network and the last sensor supply voltage.

maximum estimated number of sensors ($n_{\max} = 201$) for this setup was obtained approximately 51 Hz.

This setup makes sure that all sensor nodes sample the sensor data synchronously, and then the data is rapidly pumped to the master collecting device. Also each sensor node in the chain can be provided with identical software that considerably simplifies the design of the whole network. The exact schematics and code of embedded software of the sensor node are attached in appendices of the full version of this work.

4.3. Surface reconstruction with accelerometer and magnetometer network

The implementation and performance of the surface shape reconstruction with, accelerometer and magnetometer data proposed in Subsection 2.2 were evaluated in detail.

For surface segment orientation estimation, a sensor node based on low-power and low-cost hardware was designed. Earth gravity and magnetic field vector direction measurement was done with 3-axis accelerometer and 3-axis magnetometer LSM303DLHC. The performance of this low-cost setup in combination with TRIAD [41] algorithm was evaluated using the commercial high-precision inertial measurement unit Xsens MTi-G as a ground truth. Prior to testing, the magnetometer of LSM303DLHC was calibrated to compensate for the hard and soft iron effects according to the reference [56]. For 1000 sample measurement sequence determined RMS errors for pitch, roll, and heading angles were 1.7, 1.8, and 5.4 degrees respectively.

For shape reconstruction, a network of 63 3-axis acceleration and magnetic sensor nodes was experimentally tested [9]. Sensors were arranged in 9×7 -grid formation and sewed between two layers of fabric with mutual distances 4.8 cm lengthwise and 3.5 cm across. For convenient data acquisition, the network was connected to a master data acquisition device with a battery and a Bluetooth transceiver (Fig. 4.6) to enable data transfer to any conventional computing device such as PC, tablet or smartphone (Fig. 4.7). Total average current consumption of 63 sensor network and master data acquisition module is around 80 mA providing more than 12 hours of operation from 1000 mAh battery.



Figure 4.6. Master data acquisition module.

Left – exposed components of the module with the MSP430g2553 microcontroller and the BTM-222 Bluetooth transceiver. Right – components of the module inside 3D printed enclosure with dimensions 5.5 cm × 6 cm × 1.3 cm.

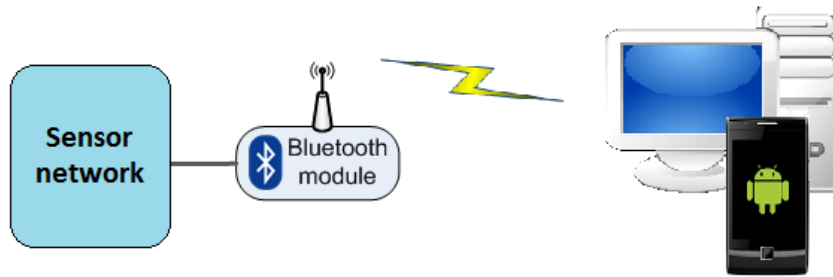


Figure 4.7. Structure of data acquisition system.

The shape reconstruction algorithm was implemented both in MATLAB environment on desktop computer and as an application on a mobile Android device to demonstrate fully portable system operation (Fig. 4.8). A video demonstration of real-time operation of the experimental setup is available in [57].

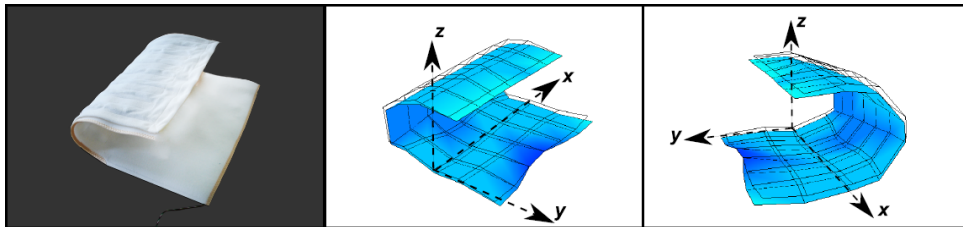


Figure 4.8. Fabric with an embedded sensor layer and corresponding reconstructed shape models in Android application.

To evaluate the accuracy of the proposed shape sensing method, an experimental setup consisting of a shape sensing sensor fabric, a Microsoft Kinect v2 (acting as a 3D scanner and used as a reference), and a desktop computer was designed (Fig. 4.9). The setup allowed to film the sensor fabric with the Kinect sensor and simultaneously acquire and compare the data from both sensors. Three different experiments were done: two in static conditions (movement acceleration $\ll g$), and one in dynamic. In each experiment, the data of at least 1000 different test shapes was obtained.

In static conditions, experiments with reference sensor located in the center and in the corner of the grid were done to observe the error distribution in the reconstructed model. Reconstruction error was expected to increase for sensor locations further away from the reference. In Fig. 4.10, the mean differences of all shapes for each sensor location are mapped on the sensor grid structure. As expected, it can be seen that mean differences are greater for points that are further

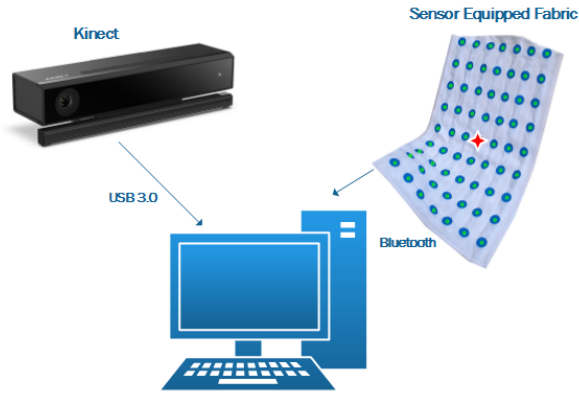


Figure 4.9. Experimental setup diagram.

On fabric, sensor locations are marked with small circles. Reference sensor location is marked with a star.

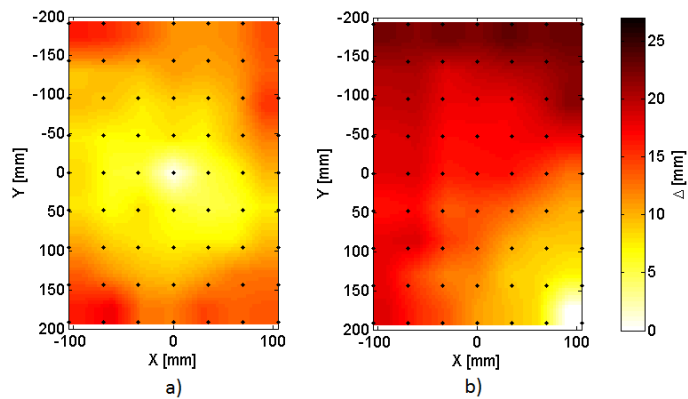


Figure 4.10. Difference maps of shape sensing sensor array in comparison to Kinect.

a) reference sensor located in the center of the grid, b) reference sensor located in the corner of the grid. The black dots indicate the locations of the sensors in the grid (points that are reconstructed).

from the reference sensor location. The distribution of mean differences for reconstruction are shown in Fig. 4.11 and Fig. 4.12. Differences and standard deviation along each axis are provided in Table 4.1. Taking the total error as Euclidean distance of standard deviations along each axis, in static conditions, the error relative to smallest surface dimension (21 cm) is obtained 6 %.

In dynamic condition experiments, a wearable vest with the back side made from the fabric with attached shape sensing sensor array was designed (Fig. 4.13 a). In front of the Kinect sensor, the subject was performing movements in speeds typical to a light workout. Similarly as in previous experiments, the data were recorded from Kinect and the sensor system (Fig. 4.13 b). The error maps and the distribution can be found in the full version of this work.

4.4. Conclusions

It was demonstrated that the basic surface shape reconstruction can be done with a 3-axis accelerometer network. Directly, acceleration sensors can not measure orientations in all three degrees of freedom limiting the ability to measure the free-form 3D shapes. This problem can be reduced with the proposed method that estimates the rotations around the vertical axis from

Table 4.1

Distribution parameters of differences between the Kinect and Shape sensing array points

	<i>X</i>	<i>Y</i>	<i>Z</i>
μ_{center} [mm]	-0.7	2.1	1.1
σ_{center} [mm]	8.9	6.7	5.8
μ_{corner} [mm]	0.1	-0.1	1.6
σ_{corner} [mm]	14.4	10.4	8.7

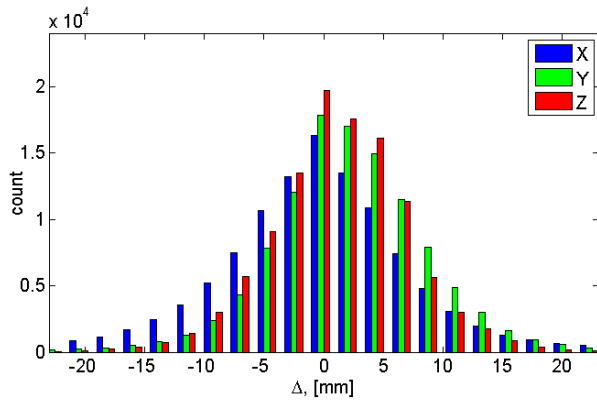


Figure 4.11. Difference distribution between points from proposed method and Kinect sensor. Reference in the center.

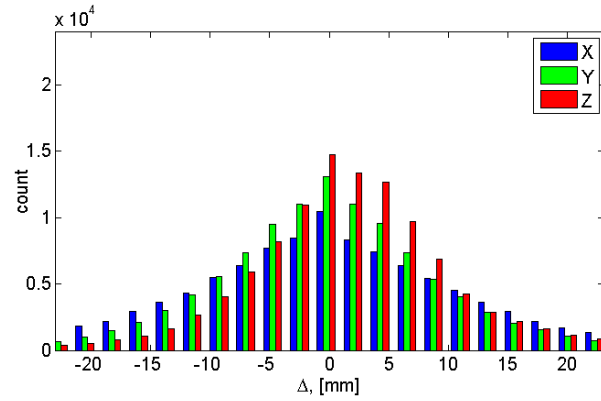


Figure 4.12. Difference distribution between points from proposed method and Kinect sensor. Reference in the corner.

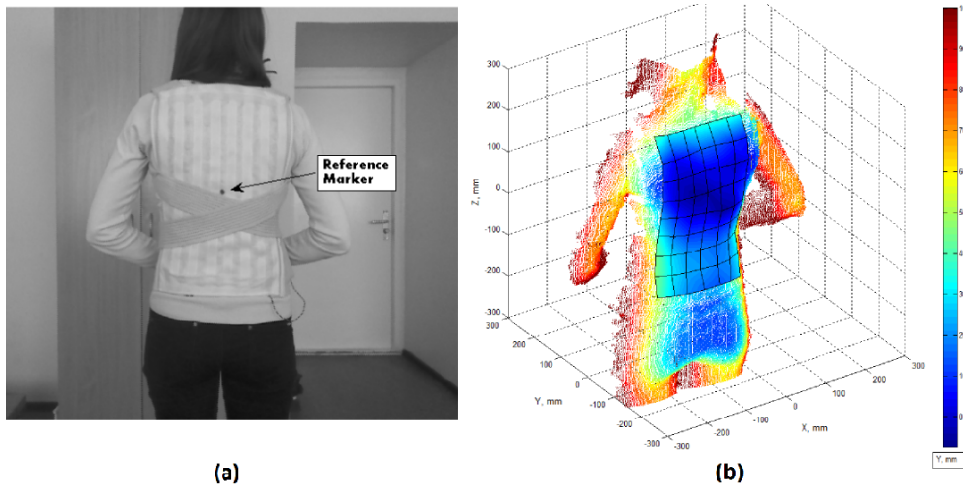


Figure 4.13. Posture monitoring experimental setup.

a) human wearing an vest with integrated shape sensing sensor array; b) superimposed models of Kinect sensor and proposed system. The colour is mapped along *y* axis to demonstrate the depth profile.

inclination measurements; however, it requires considerable computing power and still does not remove the problem completely. This suggests that for mobile CPS applications, more suitable would be some direct method that can measure the third degree of freedom of orientation such as addition of magnetometers.

The experimental test of proposed enhanced daisy-chained SPI architecture showed capability of data acquisition from more than 200 sensor nodes while maintaining a maximum sampling

frequency of the whole network around 50 Hz. The demonstrated ability to acquire the data from a low-power, low-cost sensor network is essential for mobile CPS requiring a large amount of closely spaced sensors.

The equation (3.1) suggests that reducing either the resistance of conducting wires or the current consumption of sensor nodes could significantly increase the maximum number of sensors even more. For example, reducing the wire length thus the resistance 10 times would allow connecting more than 600 sensor nodes. Up to a 17-Hz sampling frequency could still be achieved with the same hardware.

The experimental tests of 3D shape data acquisition with a 3-axis acceleration/magnetic sensor network showed the ability to reconstruct free-form 3D shapes in real-time. In static condition tests, reconstruction accuracy was achieved with an error of 6 % relative to the smallest surface dimension when compared to the Kinect v2 sensor. While sufficient for a number of applications, this error is relatively high compared to the approximation error in the simulations obtained in Subsection 2.2. These errors occur due to the sensor measurement and mounting errors (Fig. 2.7) and have a significant impact on the reconstruction accuracy.

Empirically it was found that the LSM303DLHC sensor noise level and residual calibration errors introduce a negligible impact on the shape reconstruction error. In contrast, accelerations due to movement as well as magnetic perturbations can introduce errors comparable to measured Earth gravity and magnetic field vectors. According to Fig. 2.7, this can introduce significant errors in the shape reconstruction. This problem could be reduced by applying advanced data filtering methods or adding additional sensors such as gyroscopes to assist orientation estimation; however, increased data processing complexity and power consumption have to be resolved.

Other significant error lies within mechanical mounting. It is reasonable to state that without a sophisticated manufacturing process the sensors are mounted with up to a 10-% location error (3.5 mm error for inter sensor distances of 3.5 cm) and a 5-% orientation error ($\pi/20$ angle error) leading to an increase in reconstruction error of around 0.9 % and 2.0 % respectively. This implies that during the system design, particular attention has to be paid to mechanical implementation.

5. SHAPE SENSING APPLICATION IN MOBILE CYBER-PHYSICAL SYSTEMS

5.1. Posture monitoring and feedback

To validate the proposed method practical application in mobile CPS, a complete system that can be used during daily activities for posture monitoring and biofeedback generation was developed [12]. The proposed system consists of a wearable sensor system for data acquisition and transfer and a conventional smartphone with a custom made application for sensor data processing and user interface (Fig. 5.1).

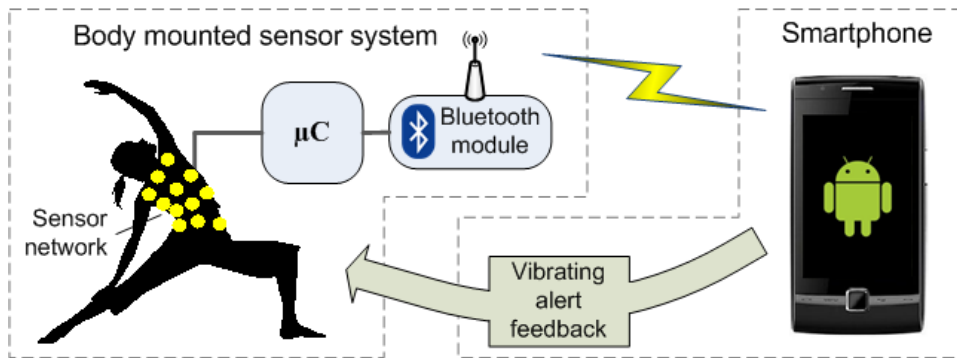


Figure 5.1. Structure of posture monitoring system.

A custom Android application for data processing, logging and feedback generation was developed (Fig. 5.2). An algorithm that compares the current state model with a previously stored correct posture model is used for decision making if feedback has to be provided. A test study was done to evaluate the proposed systems operation performance and influence on user's posture [12].

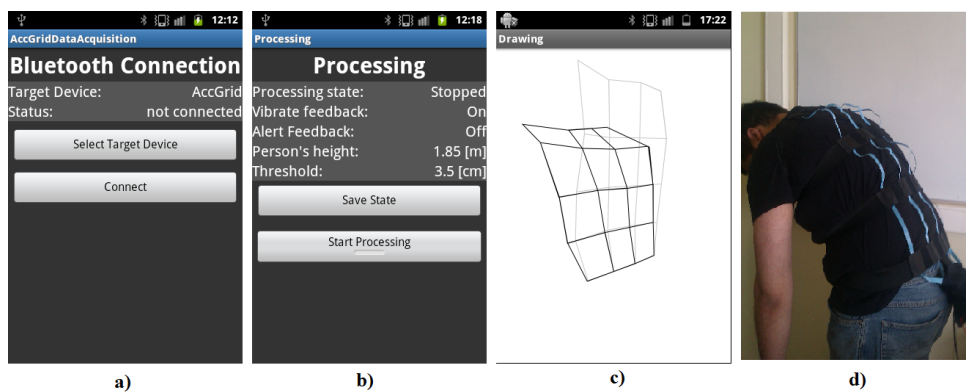


Figure 5.2. Android application screens and sensor device.

- a) screen of Bluetooth interface setup; b) screen of processing state interface; c) screen of stored and reconstructed posture models; d) wearable device.

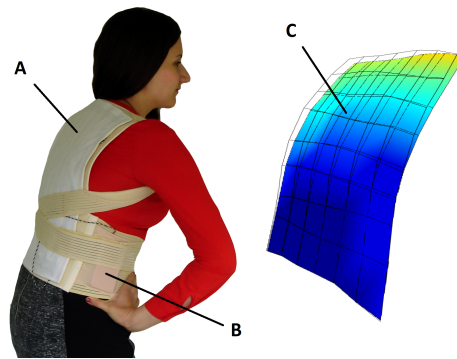


Figure 5.3. Smart wearable device for posture monitoring.

A – shape sensing fabric with an embedded accelerometer/magnetometer network; B – data acquisition module with a Bluetooth transceiver and a rechargeable lithium battery; C – posture model rendered in Android application. The color indicates the deviation from previously stored reference model indicated with a transparent grid.

5.2. Approbation and pilots for medical applications

The performance of the proposed methods operating in real-life conditions was tested during pilot studies for medical application. A number of prototype devices were built that utilize proposed shape sensing method and their application was piloted.

In "Unihaus Ltd.", the posture monitoring and feedback system described in Subsection 5.1 was piloted for patients aged from 13 to 15 with severe back posture defects. The aim of the pilot study was to validate the system applicability in orthopedics and physiotherapy.

In collaboration with the rehabilitation center "MEL", a prototype for mobile posture monitoring and feedback system was developed and piloted for application in rehabilitation of young cerebral palsy patients with upper body muscle dystonia. A smart wearable device (SWD) was developed basing on the mobile system architecture described in Subsection 5.1 and the shape sensing fabric described in Subsection 4.3 (see Fig. 5.3). The device is connected to a smartphone where a custom application provides reception of sensor data, processing, data storage, visualization, and user interface.

During the pilot study, the SWD was tested with cerebral palsy patients in close supervision of medical staff. It was used as a technical tool to assist in rehabilitation exercises to help the patient to control its upper body position and posture via the biofeedback mechanism provided by the device. In Fig. 5.4, the process of the system application in pilot study is shown. The study showed that the proposed posture monitoring and feedback system provided non-obtrusive means for posture monitoring and feedback in mobile environment without specific infrastructure.

5.3. Conclusions

The approbation and pilot tests provided that the proposed methods can be practically implemented in mobile CPS. It was demonstrated that the proposed shape sensing method that is based on orientation measurements from an acceleration/magnetic sensor network indeed can be seamlessly integrated into the smart garments. The tested conventional mobile computing devices with processor clock frequencies starting from 600 MHz were able to run the data processing application in real-time. This demonstrates that the proposed algorithms are lightweight enough to be integrated into mobile CPS with limited resources.

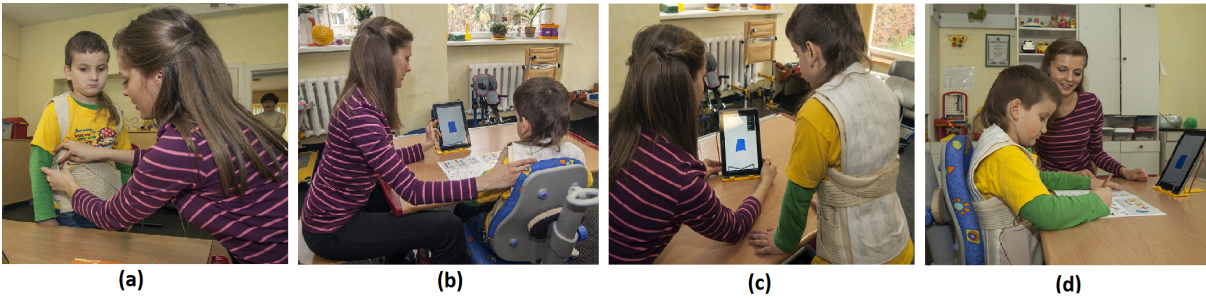


Figure 5.4. Pilot study of SWD application in the rehabilitation center "MEL".

(a) the SWD is being setup; (b) reference posture is being calibrated; (c) the features of the system is introduced to the patient; (d) training process, the system is running in background of therapy session showing real-time posture model and providing feedback if deviations from the calibrated reference model are detected.

The clear application potential of the proposed shape sensing methods is proved by the interest from medical staff, which has taken a form of collaborative publications [\[18, 19\]](#) and presentations in medical conferences. Full approbation and pilot study reviews from medical institutions can be found in the appendices of the full Thesis work. In addition, while the practically tested applications in this work are related to medicine, the author suggests that it is by no means the only suitable field of application for the proposed methods. The demonstrated ability to measure free form 3D shape in real-time with low-cost, low-power electronics can also be beneficial in other fields mentioned in the introduction of this work such as robotics, flexible devices, or high-end sports equipment.

DISCUSSION AND CONCLUSIONS

The aim of this work was to facilitate the development of new CPS applications by exploring new 3D shape sensing methods. In the literature, two distinct approaches were found for shape sensing with embedded equipment: one is based on the measurement of bending of the material, and the other utilizes the inertial/magnetic sensors. The approach with the inertial/magnetic sensors was chosen for further studies due to superior properties and advancements in MEMS technology.

In Subsection 2.1, the theoretical basis for 3D object shape measurement with accelerometer network was described. In Subsection 4.1, it was experimentally validated. The method allows only limited variations of the object shapes to be measured. The main contribution of this work regarding shape sensing methods is in the method for free-form 3D shape sensing with accelerometer/magnetometer network in Subsection 2.2. Previously proposed solutions require a high computing power therefore are not well suited for mobile CPS. A novel method for shape reconstruction was proposed that requires noticeably lower computing resources while having minor sacrifice in precision. It was identified that for shape sensing with high resolution, the use of a large number of sensors is preferable. As none of the currently available data transfer interfaces were directly suitable, a new method for data transfer was proposed in Section 3. This method was used in the experimental acceleration/magnetic sensor network described in Subsection 4.3. The network allowed obtaining the shape of the fabric in real-time using the proposed shape reconstruction method. Also a specific experimental setup was designed for detailed accuracy evaluation of the proposed shape reconstruction algorithm with a statistically reasonable data set.

The last section – Section 5 – describes the proposed method implementation in mobile CPS for medical application. In collaboration with medical specialists, the systems were piloted for medical studies. The results of these studies were published and presented in medical conferences. Despite pilots only for medical applications, the reported performance in terms that are essential for mobile CPS provides foundation for further application of proposed methods in other fields.

In conclusion, in this work the methods enabling real-time free-form 3D shape sensing with embedded equipment that are applicable in mobile CPS were proposed, experimentally tested, and successfully piloted. All of the tasks defined at the beginning of this work are successfully completed and described throughout the sections of this Thesis work; therefore, the author considers this work to be complete and finished.

BIBLIOGRAPHY

- [1] R. A. Russell and S. Parkinson. “Sensing surface shape by touch”. In: *IEEE International Conference on Robotics and Automation*. Vol. 1. 1993, pp. 423–428.
- [2] D. Trivedi and C. Rahn. “Model-based shape estimation for soft robotic manipulators: The planar case”. In: *Journal of Mechanisms and Robotics*. Vol. 6. 2. 2014.
- [3] A. Nathan et al. “Flexible Electronics: The Next Ubiquitous Platform”. In: *Proceedings of the IEEE Special Centennial Issue*. Vol. 100. 2012, pp. 1486–1517.
- [4] J. Cheng et al. “Smart Textiles: From Niche to Mainstream”. In: *IEEE Pervasive Computing*. Vol. 12. 3. 2013, pp. 81–84.
- [5] F. Chollet and H. Liu. *A (not so) short introduction to Micro Electro Mechanical Systems*. This is an electronic document published under Creative Commons Attribution-NonCommercial 3.0 License. 2015. URL: <http://memscyclopedia.org/introMEMS.html>.
- [6] E. A. Lee and S. A. Seshia. *Introduction to Embedded Systems – A Cyber-Physical Systems Approach*. Second Edition, LeeSeshia.org, 2015.
- [7] M. J. Holroyd. *Methods for the Synchronous Acquisition of 3D Shape and Material Appearance*. PhD Thesis, University of Virginia, 2011.
- [8] G. Sansoni, M. Trebeschi, and F. Docchio. “State-of-the-art and applications of 3D imaging sensors in industry, cultural heritage, medicine, and criminal investigation”. In: *Sensors*. Vol. 9. 1. 2009, pp. 568–601.
- [9] A. Hermanis, R. Cacurs, and M. Greitans. “Acceleration and Magnetic Sensor Network for Shape Sensing”. In: *IEEE Sensors Journal*. Vol. 16. 5. 2016, pp. 1271–1280.
- [10] A. Hermanis, R. Cacurs, and M. Greitans. “Shape sensing based on acceleration and magnetic sensor system”. In: *2nd IEEE International Symposium on Inertial Sensors and Systems (IEEE ISISS 2015)*. 2015.
- [11] A. Hermanis et al. “Efficient real-time data acquisition of wired sensor network with line topology”. In: *2013 IEEE Conference on Open Systems (ICOS 2013)*. 2013, pp. 133–138.
- [12] A. Hermanis et al. “Wearable Posture Monitoring System with Biofeedback via Smartphone”. In: *Journal of Medical and Bioengineering*. Vol. 2. 1. 2013, pp. 40–44.
- [13] K. Nesnebergs, A. Hermanis, and M. Greitans. “A Method for segment based surface reconstruction from discrete inclination values”. In: *Elektronika ir Elektrotechnika*. Vol. 20. 2. 2014, pp. 32–35.
- [14] A. Hermanis and K. Nesnebergs. “Grid shaped accelerometer network for surface shape recognition”. In: *Proceedings of the Biennial Baltic Electronics Conference, BEC*. 2012, pp. 203–206.
- [15] A. Hermanis. *Inerciālo sensoru tīkls virsmas formas noteikšanai*. Master’s thesis, RTU, 2012.
- [16] A. Hermanis et al. “Demo: Wearable Sensor System for Human Biomechanics Monitoring”. In: *Proceedings of the 2016 International Conference on Embedded Wireless Systems and Networks*. Graz, Austria, 2016, pp. 247–248.
- [17] A. Hermanis et al. “Wearable Sensor Grid Architecture for Body Posture and Surface Detection and Rehabilitation”. In: *Proceedings of the 14th International Conference on Information Processing in Sensor Networks*. Seattle, Washington, 2015, pp. 414–415.

- [18] A. Hermanis et al. “Wearable Head And Back Posture Feedback System For Children With Cerebral Palsy”. In: *Journal of Rehabilitation Medicine (ISSN 1650–1977)*. Vol. 47. 8. 2015, p. 777.
- [19] K. Nesenbergs et al. “Virtual Reality Rehabilitation System for Children with Cerebral Palsy”. In: *25th European Academy of Childhood Disability*. Newcastle, England, 10-12 oct, 2013.
- [20] A. Hermanis and K. Nesenbergs. “Accelerometer network for human posture monitoring”. In: *Riga Technical University 53rd International Scientific Conference*. Riga, Latvia, 2012.
- [21] E. Szelitzky et al. “Low Cost Angular Displacement Sensors for Biomechanical Applications – A Review”. In: *Journal of Biomedical Engineering and Technology*. Vol. 2. 2. 2014, pp. 21–28.
- [22] D. Preethichandra and K. Kaneto. “SAW sensor network fabricated on a polyvinylidene difluoride (PVDF) substrate for dynamic surface profile sensing”. In: *IEEE Sensors Journal*. Vol. 7. 5. 2007, pp. 646–649.
- [23] R. Balakrishnan et al. “Exploring Interactive Curve and Surface Manipulation Using a Bend and Twist Sensitive Input Strip”. In: *Proceedings of the 1999 Symposium on Interactive 3D Graphics*. I3D '99. Atlanta, Georgia, USA, 1999, pp. 111–118.
- [24] T. Kato, A. Yamamoto, and T. Higuchi. “Shape recognition using piezoelectric thin films”. In: *Proceedings of the IEEE International Conference on Industrial Technology*. Vol. 1. 2003, pp. 112–116.
- [25] C. Rendl et al. “FlexSense: A transparent self-sensing deformable surface”. In: *Proceedings of the 27th Annual ACM Symposium on User Interface Software and Technology*. 2014, pp. 129–138.
- [26] F. Lorussi et al. “Wearable, redundant fabric-based sensor arrays for reconstruction of body segment posture”. In: *IEEE Sensors Journal*. Vol. 4. 6. 2004, pp. 807–818.
- [27] W. Wong and M. Wong. “Detecting spinal posture change in sitting positions with tri-axial accelerometers”. In: *Gait and Posture*. Vol. 27. 1. 2008, pp. 168–171.
- [28] G. Hansson et al. “Validity and reliability of triaxial accelerometers for inclinometry in posture analysis”. In: *Medical and Biological Engineering and Computing*. Vol. 39. 4. 2001, pp. 405–413.
- [29] R. E. Mayagoitia, A. V. Nene, and P. H. Veltink. “Accelerometer and rate gyroscope measurement of kinematics: an inexpensive alternative to optical motion analysis systems”. In: *Journal of Biomechanics*. Vol. 35. 4. 2002, pp. 537–542.
- [30] D. Roetenberg, H. Luinge, and P. Slycke. “Xsens MVN: Full 6DOF Human Motion Tracking Using Miniature Inertial Sensors”. In: *Xsens Technologies, White Paper*. 2013, pp. 1–9.
- [31] D. Roetenberg. *Inertial and Magnetic Sensing of Human Motion*. PhD Thesis, University of Twente, 2006.
- [32] T. Hoshi, S. Ozaki, and H. Shinoda. “Three-dimensional shape capture sheet using distributed triaxial accelerometers”. In: *4th International Conference on Networked Sensing Systems*. 2007, pp. 207–212.

- [33] P. Mittendorf and G. Cheng. “3D surface reconstruction for robotic body parts with artificial skins”. In: *IEEE International Conference on Intelligent Robots and Systems*. 2012, pp. 4505–4510.
- [34] T. Hoshi and H. Shinoda. “Gravity-based 3D shape measuring sheet”. In: *SICE, 2007 Annual Conference*. 2007, pp. 2126–2131.
- [35] T. Hoshi and H. Shinoda. “Three-dimensional shape capture sheet using distributed six-axis sensors”. In: *5th International Conference on Networked Sensing Systems (INSS 2008)*. 2008, pp. 156–161.
- [36] N. Sprynski et al. “Curve reconstruction via a ribbon of sensors”. In: *Proceedings of the IEEE International Conference on Electronics, Circuits, and Systems*. 2007, pp. 407–410.
- [37] D. David and N. Sprynski. “Method and device for acquisition of a geometric shape”. In: *US Patent 9,188,422*. 2005.
- [38] M. Huard et al. “Reconstruction of quasi developable surfaces from ribbon curves”. In: *Numerical Algorithms*. Vol. 63. 3. 2013, pp. 483–506.
- [39] N. Saguin-Sprynski et al. “Surfaces reconstruction via inertial sensors for monitoring”. In: *7th European Workshop on Structural Health Monitoring (EWSHM 2014) – 2nd European Conference of the Prognostics and Health Management (PHM) Society*. 2014, pp. 702–709.
- [40] N. Sprynski, B. Lacolle, and L. Biard. “Motion capture of an animated surface via sensors’ ribbons – Surface reconstruction via tangential measurements”. In: *1st International Conference on Pervasive and Embedded Computing and Communication Systems*. 2011, pp. 421–426.
- [41] M. Shuster and S. Oh. “Three-axis attitude determination from vector observations”. In: *J Guid Control*. Vol. 4. 1. 1981, pp. 70–77.
- [42] J. Leavitt, A. Sideris, and J. E. Bobrow. “High bandwidth tilt measurement using low-cost sensors”. In: *IEEE/ASME Transactions on Mechatronics*. Vol. 11. 3. 2006, pp. 320–327.
- [43] X.-S. Ji and S.-R. Wang. “Research on the MEMS gyroscope random drift error”. In: *Yuhang Xuebao/Journal of Astronautics*. Vol. 27. 4. 2006, pp. 640–642.
- [44] D. Choukroun, I. Bar-Itzhack, and Y. Oshman. “Novel quaternion Kalman filter”. In: *IEEE Transactions on Aerospace and Electronic Systems*. Vol. 42. 1. 2006, pp. 174–190.
- [45] R. G. Valenti, I. Dryanovski, and J. Xiao. “A Linear Kalman Filter for MARG Orientation Estimation Using the Algebraic Quaternion Algorithm”. In: *IEEE Transactions on Instrumentation and Measurement*. Vol. 65. 2. 2016, pp. 467–481.
- [46] H. Fourati et al. “Complementary Observer for Body Segments Motion Capturing by Inertial and Magnetic Sensors”. In: *IEEE/ASME Transactions on Mechatronics*. Vol. 19. 1. 2014, pp. 149–157.
- [47] S. Madgwick, A. Harrison, and R. Vaidyanathan. “Estimation of IMU and MARG orientation using a gradient descent algorithm”. In: *IEEE International Conference on Rehabilitation Robotics*. 2011.
- [48] STMicroelectronics. *iNEMO inertial module: 3D accelerometer, 3D gyroscope, 3D magnetometer*. 2013, pp. 1–74.
- [49] A. Hanson. *Visualizing Quaternions*. The Morgan Kaufmann Series in Interactive 3D Technology, 2005.

- [50] C. C. Liebe. “Star trackers for attitude determination”. In: *IEEE Aerospace and Electronic Systems Magazine*. Vol. 10. 6. 1995, pp. 10–16.
- [51] I. Bar-Itzhack and Y. Oshman. “Attitude Determination from Vector Observations: Quaternion Estimation”. In: *IEEE Transactions on Aerospace and Electronic Systems*. Vol. AES-21. 1. 1985, pp. 128–136.
- [52] G. Wahba. “A Least Squares Estimate of Satellite Attitude”. In: *SIAM Review*. Vol. 7. 3. 1965, pp. 409–409.
- [53] X. Yun, E. R. Bachmann, and R. B. McGhee. “A Simplified Quaternion-Based Algorithm for Orientation Estimation From Earth Gravity and Magnetic Field Measurements”. In: *IEEE Transactions on Instrumentation and Measurement*. Vol. 57. 3. 2008, pp. 638–650.
- [54] H. Estl. “SPI interface and use in a daisy-chain bus configuration”. In: *Infineon Technologies AG, Application Note, Feb. 2002*.
- [55] H. Lee et al. “Wearable personal network based on fabric serial bus using electrically conductive yarn”. In: *ETRI Journal*. Vol. 32. 5. 2010, pp. 713–721.
- [56] J. Vasconcelos et al. “Geometric approach to strapdown magnetometer calibration in sensor frame”. In: *IEEE Transactions on Aerospace and Electronic Systems*. Vol. 47. 2. 2011, pp. 1293–1306.
- [57] A. Hermanis and R. Cacurs. *YouTube, EDI shape sensing fabric video demonstration*. 25.05.2016. URL: https://www.youtube.com/watch?v=YDG0ERF2_d8.